Verification of Tropical Storm Track Prediction in Southeast Asia Using GFS Model

Honors Thesis
Presented to the College of Agriculture and Life Sciences
Department of Earth and Atmospheric Sciences
of Cornell University
in Partial Fulfillment of the Requirements for the
Research Honors Program

by
Cheuk Yi Joseph Lee

May 2013

Research Faculty Mentor: Mark W. Wysocki

ABSTRACT

This study investigates the skill of the Global Forecast System (GFS) model in predicting tropical cyclones (TCs) tracks and intensity in SE Asia from 2007 to 2011. Data from 27 TCs passing through the grid box of 20° to 25° N and 110° to 120° E are analyzed. The GFS lowest central pressure forecast is used to determine the forecasted location of the TCs. Forecast tracks and central pressures are compared to the TC best track records produced by the Joint Typhoon Warning Center (JTWC). Average errors and biases in latitude, longitude, absolute distance and central pressure are calculated for all the TCs. The GFS forecast tracks exhibit greater longitudinal errors than latitudinal errors, as well as North and East biases relative to the observation. Elliptical forecast cone is proposed so as to visually account for the directional biases of the GFS model.

1. Introduction

By verifying and understanding the limitations of numerical weather prediction (NWP) models, meteorologists can improve their forecasts of Tropical Cyclone's (TC) tracks and intensities. In the past, TC forecasts of various models and statistical schemes, including the Navy Operational Global Atmospheric Prediction System (NOGAPS), U.K. Meteorological Office global model (UKMO) and statistical hurricane prediction scheme (SHIPS), or even the consensus of the models, in different TC basins have been evaluated using different methods of verification (Goerss et al. 2004; Elsberry et al. 2007).

This research verifies the Global Forecast System (GFS) model because it is a widely used, regularly updated and free global operational NWP model operated by the National Oceanic and Atmospheric Administration (NOAA). Southeast Asia is the region of interest due to its high population in major cities as shown in Figure 1 and Figure 2, and its active and long annual TC season.

In 2002, the National Hurricane Center (NHC) developed the concentric cone of uncertainty around the TC center, which has the radii equal to the average errors in all forecasted TC tracks over the previous 10 years, and aimed to show the potential geographic range of the projected TC (Board et al. 2007).

The NHC (2013) states, "the cone represents the probable track of the center of a tropical cyclone, and is formed by enclosing the area swept out by a set of circles along the forecast track (at 12, 24, 36 hours, etc). The size of each circle is set so that two-thirds of historical official forecast errors over a 5-year sample fall within the circle." The selected circle radii, made by the NHC (2013), defining the cones in 2013 for the Atlantic and eastern North Pacific basins are listed in Table 4. In general, forecasters adapt the circular TC forecast cone comprehensively to determine the area of uncertainty.

However, circles do not account for the directionally biased uncertainty made by the models or the forecasters, in which ellipses would be a more precise choice of graphical presentation to solve this problem. Ellipses of error distribution in verifying TC forecast errors have been made before (Fogarty and Bowyer 2008), which had suggested that the elliptical graphical presentation of TC forecast uncertainty is more effective than the traditional circular forecast cone.

The major objective of the research is to assess the reliability of the GFS model's TC track and intensity forecast by evaluating the statistical error and bias. A scheme of GFS-model-based elliptical TC forecast cone is also introduced. This research would act as a reference for forecasters to forecast TCs in Southeast Asia and contribute in improving TC forecasts.

2. Methodology

In this study, only the TCs that passed through the grid box 20° to 25° N, 110° to 120° E in west Pacific Ocean during 2007 to 2011 were selected, as presented in Figure 1. The observed TC tracks, which were obtained from the best track data from the Joint Typhoon Warning Center (JTWC), and were compared to the forecast tracks from the GFS model output. There are 27 chosen TCs in total, according to the categorization provided in the best track data from the JTWC. All of them were tropical depressions, 23 TCs were tropical storms and 14 TCs were typhoons. In this research, stronger TCs are defined as the TC observations reaching the intensities of typhoon stage or even strong typhoon stage, which made up more than half of the TC samples. All of the 14 stronger TCs eventually reduced their strength and ended as weaker TCs. The summary of the data set is presented in Table 1.

All the TCs are also divided into 2 categories, those with wave-like patterns, which looped in the same region for consecutive initializations, and the non-wave-like cases. Among all the TCs, 4 of them, including Typhoon Linfa in Figure 5, had wave-like patterns. The GFS model had problems in tracking them, therefore some of the analyses would classify them as a group of outliers.

The GFS outputs initialized every 12 hours, with 6-hour intervals between each point of the TC location, over a forecast period up to 7.5 days, were used. Points of the local lowest pressure represent the locations of the TCs' centers in the target region. To avoid erratic forecasted TC tracks, an upper limit of 2.5° latitude and longitude of TC movement within 6-hour intervals is imposed on plotting the lowest pressure in the local area of interest. Among the total of 385 initializations, only 3 of them did not involve any TC observations of weak intensities.

Errors of every initialization are calculated by subtracting the GFS forecast position and central pressure from the observed TC position and central pressure. Errors in

distance are calculated using the great circle formula:

$$D = 2 \times R \times \arcsin\left(\sqrt{\left(\frac{1}{2}\sin(\phi_o - \phi_f)\right)^2 + \cos(\phi_o) \times \cos(\phi_f) \times \left(\frac{1}{2}\sin(\lambda_o - \lambda_f)\right)^2}\right)$$

D: Distance between two locations
R: Radius of Earth, R = 6371 km
ϕ_o: Latitude of observed position in degrees
ϕ_f: Latitude of forecast position in degrees
λ_o: Longitude of observed position in degrees
λ_f: Longitude of forecast position in degrees

Errors are presented in terms of total distance, north-south distance (latitude), east-west distance (longitude), and central pressure. Each set of error values are divided into two categories, stronger TCs and weaker TCs, according to the observed TC intensities at the observed time. After averaging the magnitude of errors and the actual errors in the two categories for each TC, the mean absolute errors and the mean biases of all TCs are determined respectively. Analyses excluding Typhoon Linfa and other wave-like TCs reveal the GFS model has difficulties on forecasting their tracks. The average errors and biases are listed in Table 2 and Table 3.

In order to develop the TC forecast cone, the absolute errors and biases of distance and pressure are averaged at the initialization, 24-hour, 48-hour, 72-hour and 96-hour for each TC. Five of the TCs did not exist long enough for the GFS model to generate the 96-hour forecast. The mean absolute errors and the mean biases in different forecast periods are found after averaging the errors among all TCs, which are presented in Table 5 and Table 6.

3. Results

In Table 2, for all the TCs studied, the GFS model has slightly smaller absolute distance errors in tracking weaker TCs. The GFS model yields larger distance errors in the east-west direction than in the north-south direction in both categories. It shows the GFS model has larger uncertainty in determining the longitudinal position of a TC. The GFS forecasts also have significantly greater errors of about 35 hPa in determining TC

central pressures for stronger TCs.

From Table 3, the GFS forecasts demonstrate north and east biases on average among all TCs, as well as an underestimation of TC strength. The bias in longitude is notably larger than the bias in latitude. Compared to the stronger TCs, the GFS forecasts exhibit smaller biases in latitude, longitude and central pressure for weaker TCs. Figure 3 is an example illustrating the biases, based on the observation track and the forecast track of Typhoon Nesat, which lasted from 00Z 23 to 18Z 30 September 2011. Figure 4 also shows a forecast track of Nesat initialized at its mature stage. Both initializations show the GFS model captured Nesat's track very well in the beginning 6-hour periods, no matter before or after it became a typhoon.

The GFS model yielded extraordinary distance errors on forecasting Typhoon Linfa. Therefore, excluding Linfa, which has a wave-like structure, in the analysis, the absolute distance errors and biases of the GFS forecasts are remarkably improved. The GFS forecast errors for the other 3 TCs with wave-like pattern are similar to the forecast errors for rest of the selected TCs. Therefore, Linfa can be inferred as an outlier that causes huge difficulties for the GFS model to locate its track. The observed wave-like pattern of Typhoon Linfa, which persisted from 06Z 13 to 12Z 22 June 2009, is illustrated in Figure 5.

The longitudinal errors become significantly larger than the latitudinal errors in later forecast periods, as shown in Table 5. From the 48-hour forecast period onwards, the longitudinal errors are greater than the latitudinal errors by almost a factor of 2. The pressure errors are consistent among different forecast periods, since the GFS model tends to substantially overestimate the TC central pressure values for stronger TCs. The circular GFS forecast cone shown in Figure 6, is based on the average absolute errors of various forecast periods in Table 5, which is less skillful compared to the NHC forecast errors in Table 4.

From Table 6, there are very weak South and West forecast biases at initialization. For later forecast periods, the GFS model exhibits amplifying North and East biases. The underestimation of the TC strength is steady for different the forecast periods.

4. Discussion

Results indicate that the GFS TC forecasts yield average distance errors in a range of 300 to 350 km (in radius), which is less than half of the distance from Hong Kong to Taipei (808 km). Qualitatively speaking, the GFS model handles TC track forecasts better for normal cases than for wave-like cases.

Beta effect related processes and other tropical factors (Carr and Elsberry 2000a) could explain why the GFS model yields larger absolute longitudinal errors than absolute latitudinal errors. Mid-latitude circulation influences (Carr and Elsberry 2000b) can justify the magnifying errors when the poleward moving TCs enter the mid-latitudes. The GFS model also has problems on capturing the relocated vortex vertical structure, which causes inaccurate interactions between the upper atmosphere and the TCs (Payne et al. 2007). This flaw of the GFS model could explain the errors and biases.

Tron and Snyder (2012) concluded that "the uncertainty in best-track position and intensity are not trivial". The TC intensity uncertainty is particularly significant due to undersampling. The errors calculated from the previous analyses can be partly explained by the possible inaccuracy in the best-track data from the JTWC, especailly for the central pressure data. The JTWC might have overestimated the strength (understated the central pressure) of TCs, especially the more powerful ones, which leads to the substantial pressure errors of the GFS forecasts.

Applying the circular forecast cone graphing method of the NHC, a green forecast cone of the GFS model, using the average absolute distance errors of the 24-hour, 48-hour and 72-hour forecasts as radii, is plotted along the observation track of typhoon Neoguri in Figure 6. Positions 5, 9, 13 and 17 are the initialization, 24-hour, 48-hour and 72-hour locations of Neoguri respectively, which are the centers of the absolute error circles. The cone is constructed by connecting the tangential points of the absolute error circles. In general, the forecasting cone covers the GFS track. For example, the circle centered at observation position 9 covers the GFS forecast position 9. This GFS initialization of Neoguri is an example of weak south and west bias in later stage, which is different from the average biases in Table 3 and Table 6.

From the results above, the average distance errors in the east-west direction (longitudinal error) are much larger than the errors in the north-south direction

(latitudinal error). The traditional method of using circles to represent the directionally unbiased uncertainty is not significant enough to visually show the higher confidence of the GFS model in forecasting TC tracks in the north-south direction than in the east-west direction. Therefore, in Figure 8, Figure 9 and Figure 10, ellipses, instead of circles, are graphed based on the different longitudinal and latitudinal errors in TC track forecasts. The major and minor axes of the ellipses are in the east-west and north-south directions respectively. Although the shape of the whole elliptical forecast cone depends on the moving speed of a TC, the shapes and the axes of the average error ellipses would not change.

The GFS model is inaccurate in locating the initial positions of the TCs, and the ellipses of the minimum, average and maximum initialization errors of all TCs are plotted in Figure 7. The GFS model was relatively precise in locating the initial position of typhoon Nesat, therefore it has the minimal initialization errors among all 27 TCs, which is represented by the green ellipse. The blue ellipse indicates the average initialization errors of all GFS initializations.

The GFS model produced the greatest initialization error among all TCs in the case of a tropical depression, which was passing through the northeast part of the targeted region from 11 to 14 July 2009. The purple ellipse represents the errors of this outlier. The possible reason why the GFS model had difficulties in locating the starting positions of the tropical depression is because there were a tropical storm, Soudelor, affecting the southwest part of the area of interest at the same time (8 to 12 July 2009) and a typhoon, Molave, which crossed over the targeted region soon after the depression (15 to 19 July 2009). The average forecast distance error of the depression for the initialization positions is large, but the errors for the rest of the track are normal, which are similar to the averages of all the TCs. Therefore, multiple TCs observed in the same region during the same time period may cause problems to the GFS model in locating the initial positions of weaker TCs, but not the rest of the forecast positions.

Figure 8 shows the green elliptical forecast cone of the average longitudinal and latitudinal errors, including the initialization, 24-hour, 48-hour, 72-hour and 96-hour error ellipses, using Typhoon Neoguri as an illustration. Compared to the circular forecast cone in Figure 6, the uncertainty of forecast tracks, which corresponds to the area of the ellipse, is notably reduced.

As the GFS model made precise track forecast for typhoon Nesat, the elliptical forecast cone averaging the directional forecast errors in this particular TC is plotted on Figure 9. The narrow minor axis of the ellipses in the north-south direction exhibits the great confidence of the GFS model in locating the latitude positions of Nesat.

Figure 10 displays the same elliptical forecast cone as Figure 8, with a dashed blue hypothetical TC track based on average biases. Since the GFS model has north and east biases in initialization, 24-hour, 48-hour, 72-hour and 96-hour forecasts, the hypothetical track is linked between the biased forecast positions corresponding to the respective observation locations, which is north and east of the possible observation track on average.

5. Conclusion

In this article, the TC track and intensity forecasts of the GFS model have been verified. On average, the GFS model yields larger longitudinal errors, underestimates TC strengths and has north and east bias. Elliptical forecast cone is recommended for operational use to replace traditional circular forecast cone.

Based on the pervious graphical analysis, forecasters can easily locate a projected TC track with the uncertainty ellipses at the south and west of a corresponding GFS forecast track. Compared to the traditional directionally unbiased TC track forecast represented by circular TC forecast cones, the GFS model has higher uncertainty in forecasting the longitudinal positions of TCs, therefore TC warnings should be issued for a large area along the South China coast when TCs are approaching to the region by the GFS model guidance.

During active TC months, forecasters should be aware that the GFS model might have significant errors in locating the initial positions of the TCs when there are multiple TCs in the same area during the same period. Further research verifying TC forecast errors in multiple coexisting TCs conditions has to be conducted in order to conclude a statistically significant argument.

Future work includes determining the actual effects of the Coriolis parameter in TC forecasting in the GFS model, analyzing the relationship between the number of landfalls and the GFS model forecast accuracy, and evaluating how TC recurvature affects the

forecast skills of the GFS model. With a bigger sample size in multiple regions, a more conclusive probabilistic forecast cone can be attained.

6. Acknowledgement

The authors are grateful to receive research funding from Dr. Robert Morley via the Morley Student Research Grant from College of Agriculture and Life Sciences, Cornell University. The authors thank Mr. Brian Belcher and Mr. Marty Sullivan for their help and assistance in technical support.

REFERENCES

Broad, K., A. Leiserowitz, J. Weinkle, M. Steketee, 2007. Misinterpretations of the "cone of uncertainty" in Florida during the 2004 hurricane season. *Bulletin of the American Meteorological Society*, **88**, 651–667.

Carr, L. E., III, and R. L. Elsberry, 2000a. Dynamical tropicalcyclone track forecast errors. Part I: Tropical region errors. *Weather and Forecasting*, **15**, 641–661.

Carr, L. E., III, and R. L. Elsberry, 2000b. Dynamical tropical cyclone track forecast errors. Part II: Midlatitude circulation influences. *Weather and Forecasting*, **15**, 662–681.

Elsberry, R. L., T. D. B. Lambert, M. A. Boothe, 2007. Accuracy of Atlantic and Eastern North Pacific Tropical Cyclone Intensity Forecast Guidance. *Weather and Forecasting*, **22**, 747–762.

Fogarty C. and P. Bowyer, 2008. *An analysis of along- and cross-track forecast errors and error biases for TCs in the Atlantic Basin*. Retrieved from American Meteorological Society, 28th Conference on Hurricanes and Tropical Meteorology, website: https://ams.confex.com/ams/28Hurricanes/techprogram/paper_137458.htm

Goerss, J. S., C. R. Sampson, J. M. Gross, 2004. A History of Western North Pacific Tropical Cyclone Track Forecast Skill. *Weather and Forecasting*, **19**, 633–638.

National Hurricane Center (NHC), 2013. *Definition of the NHC track forecast cone*. Retrieved 3 March, 2013, from http://www.nhc.noaa.gov/aboutcone.shtml

Payne, K. A., R. L. Elsberry, M. A. Boothe, 2007. Assessment of Western North Pacific 96- and 120-h Track Guidance and Present Forecastability. *Weather and Forecasting*, **22**, 1003–1015.

Torn, R. D., and C. Snyder, 2012. Uncertainty of Tropical Cyclone Best-Track Information. *Weather and Forecasting*, **27**, 715–729.

United Nations Office for the Coordination of Humanitarian Affairs (OCHA), 2013. *Population Density of Asia-Pacific as per the 2008 Landscan dataset*. Retrieved 29 March 2013, from http://www.unocha.org/roap/maps-graphics/regional-reference-maps

Tables and Figures

TABLE 1. Summary of the TC strength, the corresponding sample sizes and GFS initializations.

	TC samples	GFS Initializations
All cases	27	385
Weaker than typhoon	27	382
Stronger than typhoon	14	192

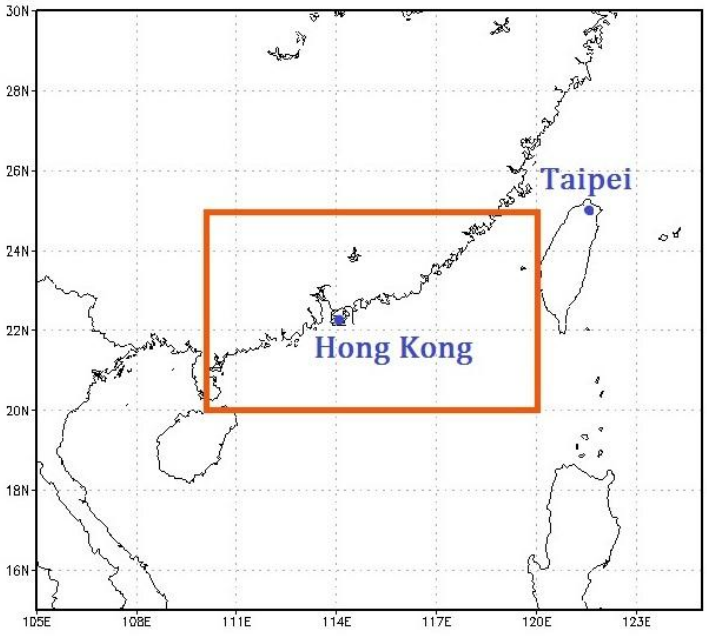

FIGURE 1. The area of interest is bounded by the orange box. It covers a large metropolitan area in South China including Hong Kong, Macau and Guangzhou.

TABLE 2. Summary of the average absolute errors of different TC strengths in latitude, longitude, absolute distance and pressure.

TC weaker than typhoon

	Lat error	**N-S distance error**	**Lon error**	**E-W distance error**	**Absolute distance error**	**Pressure error**
All TCs	1.42°	157.45 km	2.29°	236.85 km	311.36 km	7.639 hPa
Without typhoon Linfa	1.34°	148.59 km	2.22°	229.97 km	299.82 km	7.625 hPa
Without wave-like TCs	1.3°	144.07 km	2.16°	223.27 km	292.12 km	7.482 hPa

TC stronger than typhoon

All TCs	1.4°	155.61 km	2.74°	286.04 km	347.37 km	35.106 hPa
Without typhoon Linfa	1.08°	119.96 km	2.45°	256.47 km	297.76 km	35.723 hPa
Without wave-like TCs	1.12°	124.09 km	2.56°	268.47 km	311.38 km	35.257 hPa

TABLE 3. Summary of the average biases of different TC strengths in latitude, longitude and pressure.

TC weaker than typhoon

	Lat error	**N-S distance bias**		**Lon error**	**E-W distance bias**		**Pressure bias**	
All TCs	-0.27°	-30.16 km		-1.51°	-156.72 km		-3.5 hPa	
Without typhoon Linfa	-0.15°	-16.71 km	North	-1.42°	-148.13 km	East	-3.429 hPa	Under-estimate
Without wave-like TCs	-0.11°	-12.74 km		-1.34°	-139.13 km		-3.252 hPa	strength

TC stronger than typhoon

All TCs	-0.82°	-91.54 km		-2.33°	-244.08 km		-35.026 hPa	
Without typhoon Linfa	-0.46°	-51.14 km	North	-2.09°	-218.94 km	East	-35.636 hPa	Under-estimate
Without wave-like TCs	-0.47°	-52.15 km		-2.21°	-232.2 km		-35.155 hPa	strength

TABLE 4. Radii of NHC forecast cone circles for 2013, based on error statistics from 2008-2012 (NHC 2013).

Forecast Period	2/3 Probability Circle, Atlantic Basin	2/3 Probability Circle, Eastern North Pacific Basin
24 hours	96.304 km	90.748 km
48 hours	170.384 km	151.864 km
72 hours	237.056 km	205.572 km
96 hours	327.804 km	290.764 km

TABLE 5. Summary of the average absolute errors of different forecast periods in latitude, longitude, absolute distance and pressure.

Forecast Period	Lat error	N-S distance error	Lon error	E-W distance error	Absolute distance error	Pressure error
Initialization	0.53°	58.72 km	0.61°	64.53 km	98.01 km	14.25 hPa
24 hours	0.76°	84.06 km	1.03°	108.99 km	152.53 km	17.07 hPa
48 hours	1.08°	120.52 km	2.09°	219.93 km	267.68 km	21.24 hPa
72 hours	1.39°	154.51 km	3.32°	348.15 km	404.46 km	24.35 hPa
96 hours	2.12°	235.50 km	4.85°	507.19 km	594.42 km	24.74 hPa

TABLE 6. Summary of the average biases of different forecast periods in latitude, longitude and pressure.

Forecast Period	Lat bias	N-S distance bias		Lon bias	E-W distance bias		Pressure bias	
Initialization	+0.01°	+1.58 km	South	+0.04°	+3.98 km	West	-12.12 hPa	
24 hours	-0.20°	-21.64 km		-0.69°	-73.15 km		-14.52 hPa	Under-estimate strength
48 hours	-0.56°	-62.23 km	North	-1.64°	-172.53 km	East	-18.08 hPa	
72 hours	-0.83°	-91.86 km		-2.66°	-279.05 km		-20.47 hPa	
96 hours	-1.40°	-155.24 km		-4.03°	-421.66 km		-20.58 hPa	

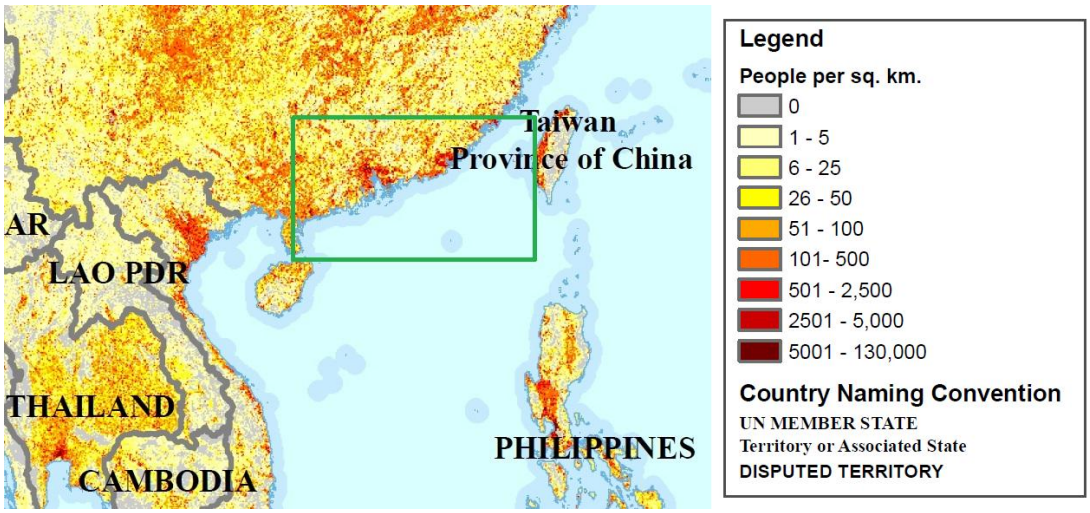

FIGURE 2. An extract of the population density map as per 2008 Landscan dataset made by the United Nations Office for the Coordination of Humanitarian Affairs (OCHA 2013). The area of interest is bounded by the green box superimposed on the population density map of SE Asia. The high population density shows the social implications of improving TC forecasts.

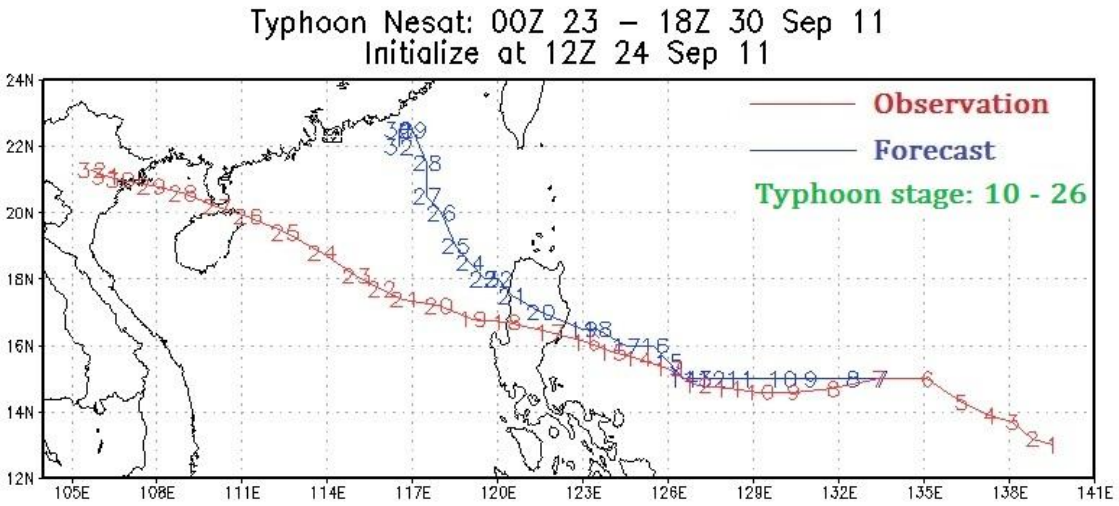

FIGURE 3. 24 September 2011 12Z (position 7) initialization: GFS forecast track shows north and east bias compared to the observation. The distance errors in the east-west direction are larger than the distance errors in the north-south direction. Absolute distance errors increase over time.

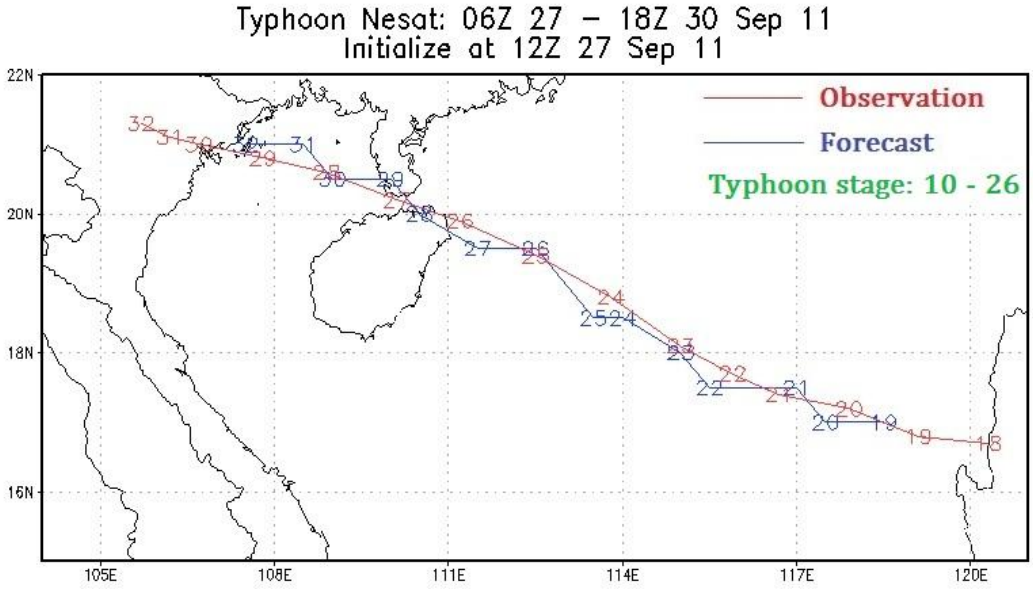

FIGURE 4. 27 September 2011 12Z (position 19) initialization: GFS forecast track shows an excellent qualitative alignment with the observation in track direction. Distance errors grow after 36 hours (after position 24 in the graph) when Nesat weakens.

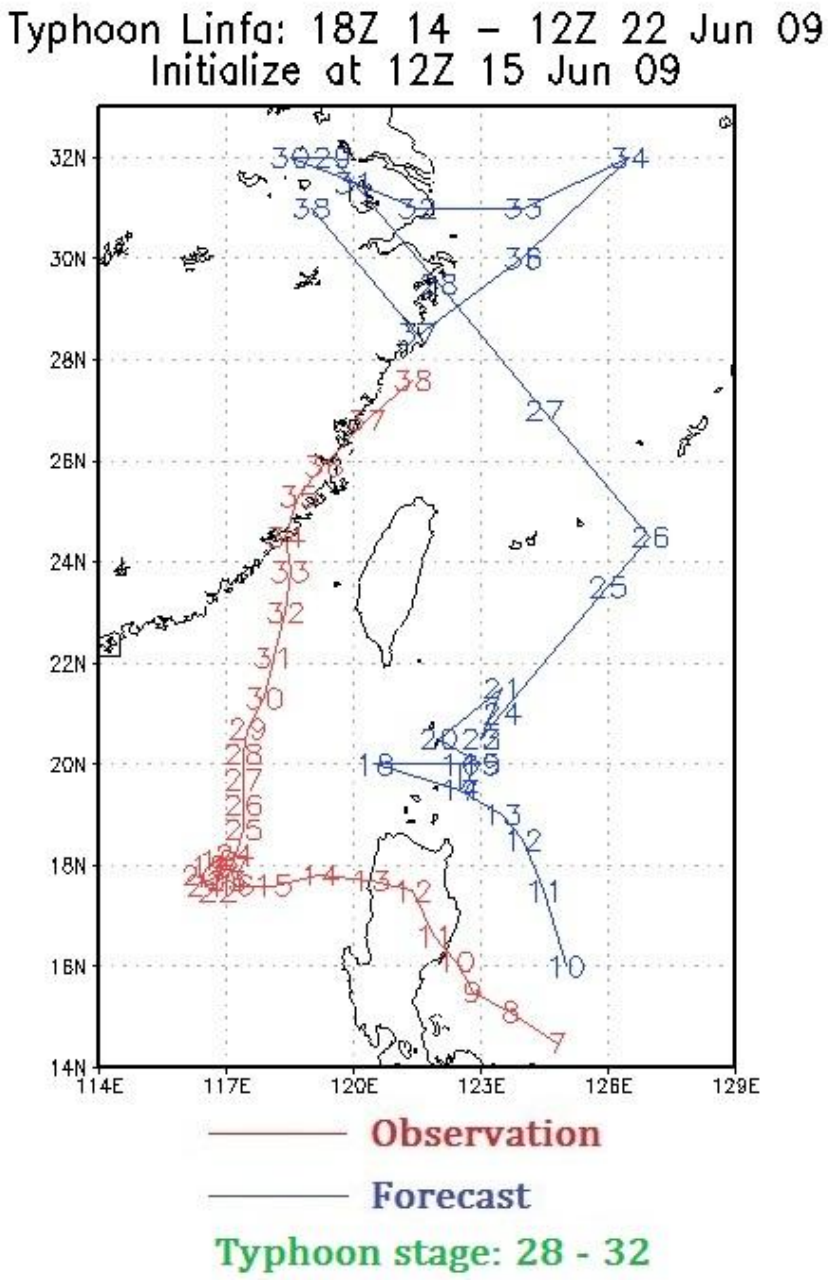

FIGURE 5. 15 June 2009 12Z (position 10) initialization: Typhoon Linfa exhibited a wave-like pattern for over 2 days (position 16 to position 24). The GFS forecast track qualitatively captures the wave-like pattern, however the absolute distance errors are greatly magnified after the looping, which greatly reduce the forecast accuracy quantitatively. Excluding Linfa, the average absolute errors and biases are greatly improved, as listed in Table 2 and 3.

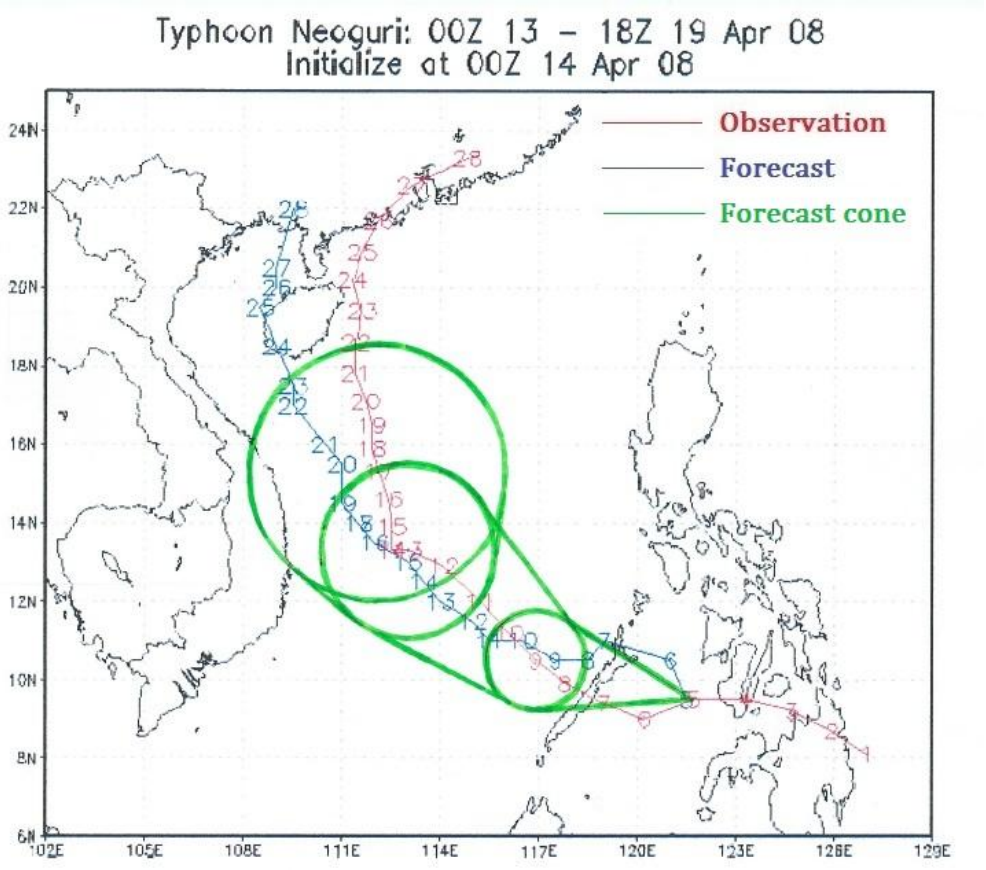

FIGURE 6. 14 April 2008 00Z (position 5) initialization: Circular forecast cone based on the mean absolute distance error of all TCs are plotted at the 24-hour (position 9), 48-hour (position 13) and 72-hour (position 17) after the initialization, centered at the observed track. Corresponding forecast locations are within the cone in general, except for the every early stage. This particular initialization displays a weak south and west bias in later stage.

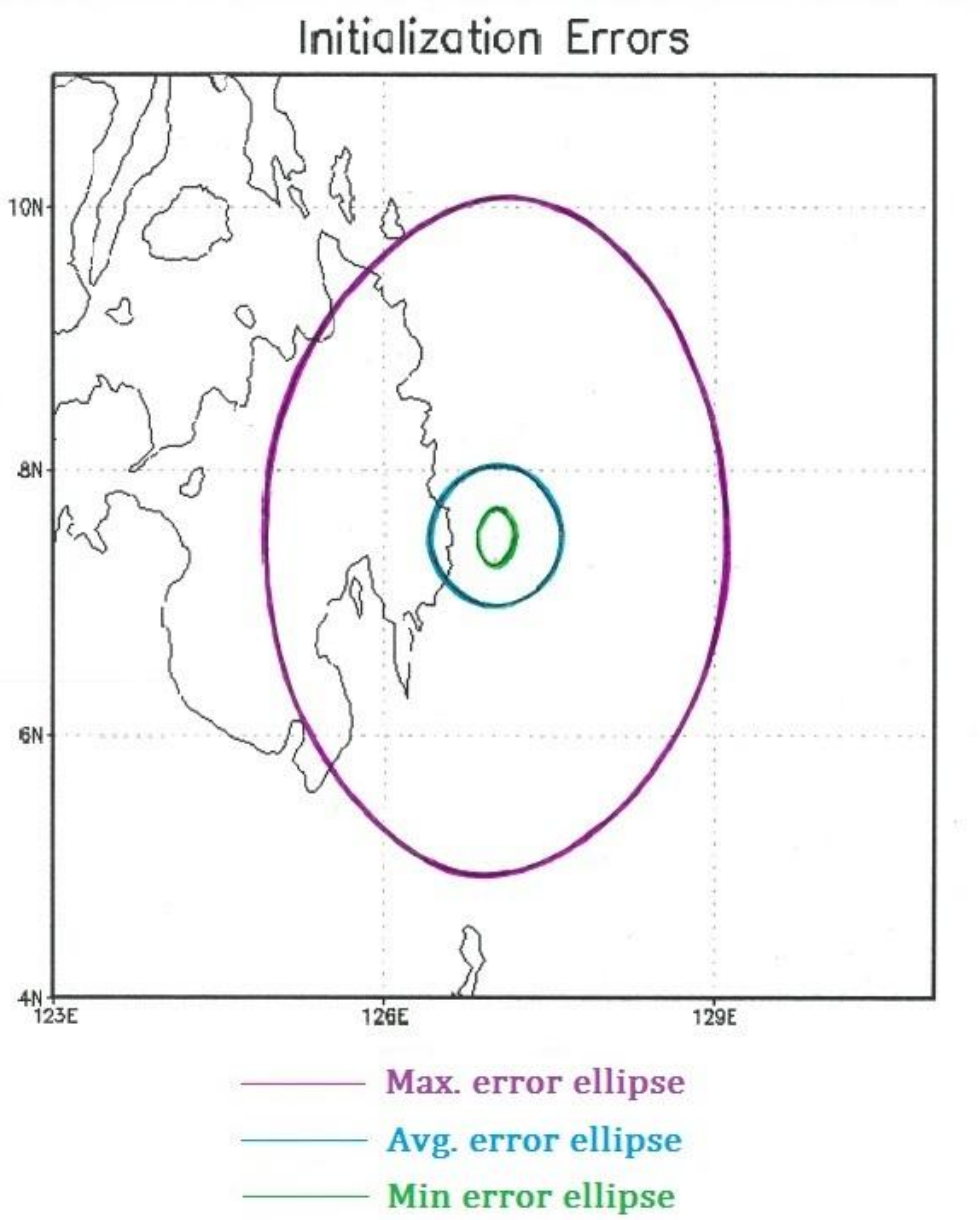

FIGURE 7. The green minimum initialization error ellipse is drawn according to the average initialization errors of Typhoon Nesat; The blue ellipse is the average initialization error ellipse of all cases (see Table 5); The purple maximum initialization error ellipse is drawn according to the average initialization errors of the tropical depression lasted from 11 to 14 July 2009. All three of the initialization ellipses are drawn without accounting for directional biases.

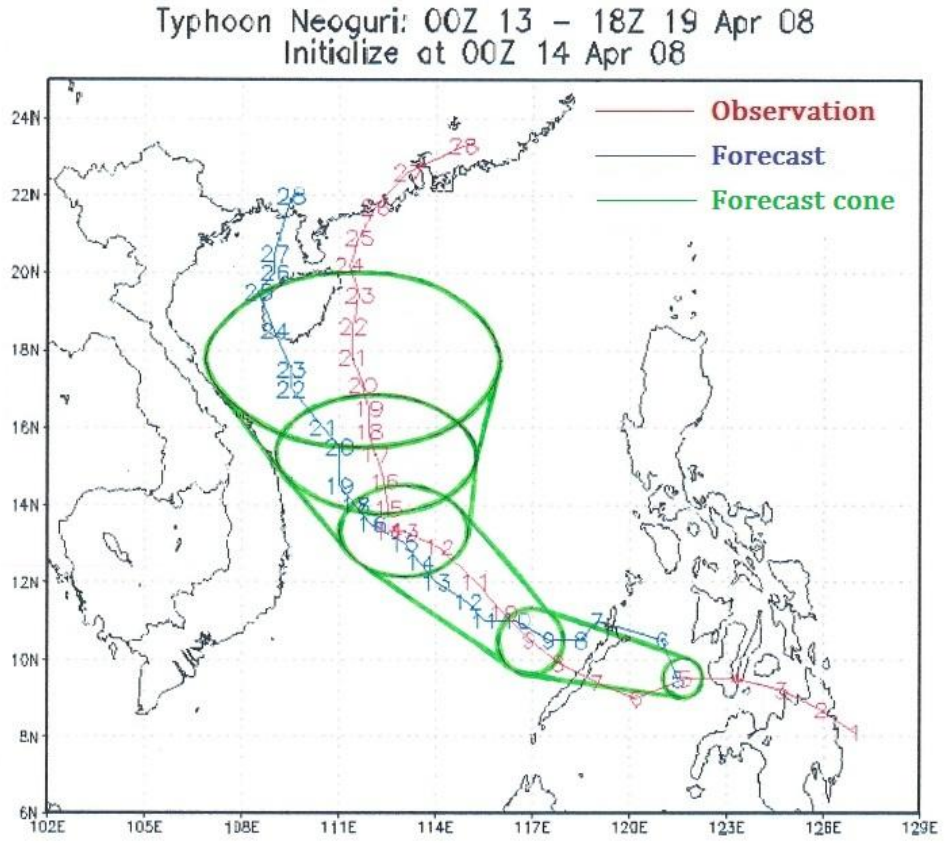

FIGURE 8. The elliptical forecast cone consists of 5 ellipses representing the directional average errors of the initialization (position 5), 24-hour (position 9), 48-hour (position 13), 72-hour (position 17) and 96-hour (position 21) forecast. The elliptical forecast cone is relatively more accurate in locating TCs since it is smaller than the circular one in Figure 6. The elliptical forecast cone shows relatively higher forecast uncertainty in the longitudinal direction.

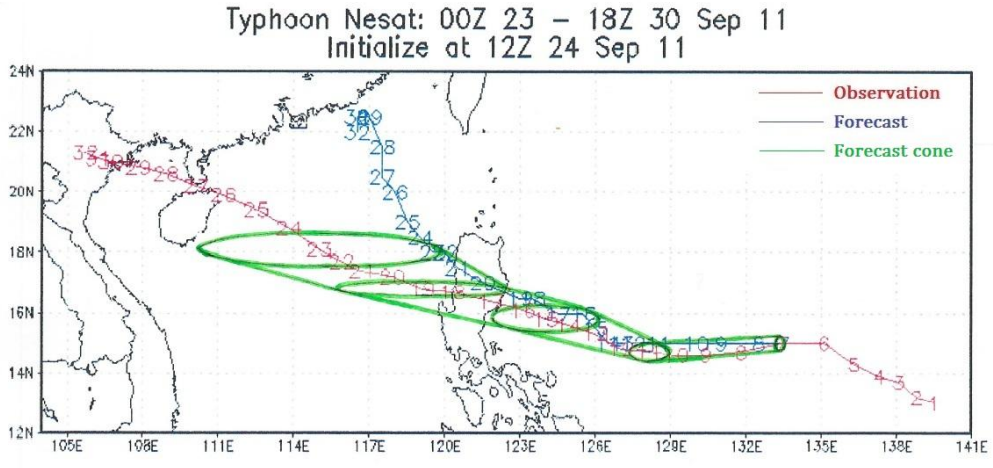

FIGURE 9. Similar to Figure 8, the elliptical forecast cone is based on the mean errors of Typhoon Nesat in particular. Since the GFS model is accurate in determining the latitudinal positions of Nesat, the ellipses are relatively narrow in the north-south direction compared to Figure 8.

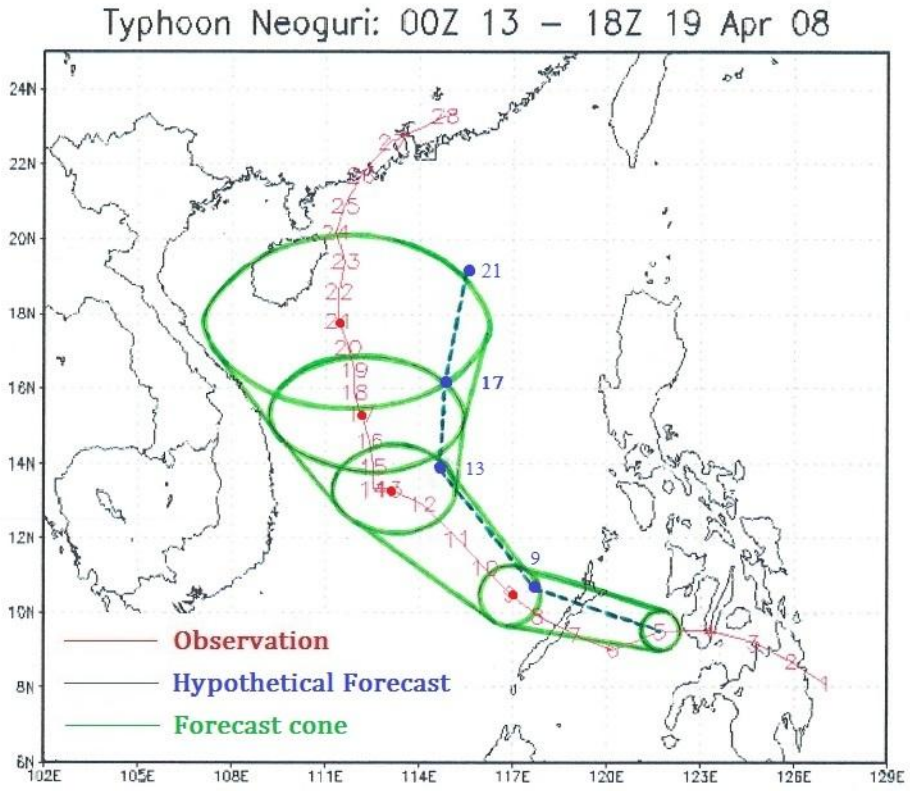

FIGURE 10. A hypothetical GFS forecast TC track, which accounted for the mean biases relative to the observations, is plotted with the same elliptical forecast cone in Figure 8, representing the mean absolute errors. Given a GFS forecast TC track, forecasters should expect the corresponding centers of forecast uncertainty ellipses to be located at the south and west of the TC.